JOURNAL OF THE
ELECTRON DEVICES SOCIETY

Received 27 August 2022; revised 3 October 2022; accepted 10 October 2022. Date of publication 12 October 2022; date of current version 26 October 2022.
The review of this article was arranged by Editor Shuji Ikeda.

Digital Object Identifier 10.1109/JEDS.2022.3214299

Ferroelectric Polarization Enhancement in Hafnium-Based Oxides Through Capping Layer Engineering

HSUAN-HAN CHEN [1], **RUO-YIN LIAO** [1], **WU-CHING CHOU** [1], **HSIAO-HSUAN HSU** [2], **CHUN-HU CHENG** [3], **AND CHING-CHIEN HUANG** [4]

1 Department of Electro-Physics, National Yang Ming Chiao Tung University, Hsinchu 30010, Taiwan
2 Institute of Materials Science and Engineering, National Taipei University of Technology, Taipei 10608, Taiwan
3 Department of Mechatronic Engineering, National Taiwan Normal University, Taipei 10610, Taiwan
4 Department of Mechanical Engineering, National Kaohsiung University of Science and Technology, Kaohsiung 80778, Taiwan

CORRESPONDING AUTHORS: C.-H. CHENG and H.-H. HSU (e-mail: chcheng@ntnu.edu.tw; hhhsu@mail.ntut.edu.tw)

This work was supported by the Ministry of Science and Technology, Taiwan, under Grant MOST 110-2221-E-003-024-MY2.

ABSTRACT In this work, we investigate that the capping layer (CL) engineering of aluminum oxide (AlO_x) on the dopant-free hafnium oxide (HfO_x) and the hafnium zirconium oxide ($HfZrO_x$) ferroelectric metal-ferroelectric-metal (MFM) capacitors. The AlO_x CL featuring large bandgap and excellent thermal stability offers a stable interface favorable for ferroelectric phase transition. Therefore, the ferroelectric polarization and high-temperature leakage current of $HfZrO_x$ MFM capacitor can be largely improved due to the combination of zirconium doping and AlO_x capping effect. From the analysis of interface thermodynamic stability and leakage current mechanism, the AlO_x CL effectively alleviates interface defect traps between electrode and ferroelectric $HfZrO_x$, which lowers high-temperature leakage current, reduces ferroelectric domains pinning, enhances ferroelectric polarization, and stabilizes the long-term endurance cycling.

INDEX TERMS Ferroelectric, aluminum oxide, hafnium zirconium oxide, power consumption.

I. INTRODUCTION

To support the rapid development of neuromorphic systems, artificial intelligence chips and Internet of Thing (IoT) technologies, the ferroelectric random-access memory and ferroelectric field-effect transistor attract more attention and are the promising candidate for the applications of next-generation memory [1], [2], [3] and in-memory computing [4]. Recently, the HfO_2-based ferroelectric materials have been widely investigated to replace the conventional ferroelectric perovskites, owing to the potential advantages including low-power consumption, fast switching speed, high device scalability and complementary-metal-oxide-semiconductor friendly process [5], [6], [7], [8], [9], [10]. According to the previous works, using the dopants (Aluminum, Zirconium, etc.) [6], [7], [8], [9], [10], [11], [12], [13], [14], [15], [16], [17], [18], [19] and metal gate stress engineering [20], [21] to stabilize the formation of the non-centrosymmetric orthorhombic phase transition are common-used approaches to achieve the ferroelectricity properties in HfO_2 film. It is worth to note that the ferroelectric $HfZrO_x$ films with ~50% Zr doping ratio have successfully achieved the favorable ferroelectric phase transition, well-behaved ferroelectric polarization property and steep switched transistor with negative capacitance operation [15], [16], [17], [18], [19]. However, the requirement of slight element doping into HfO_2 possibly causes an undesired fluctuation on the device performance while the film thickness is continuously scaled down. The imprecise element doping in HfO_2 would affect the formation of ferroelectric orthorhombic phase during annealing and also increase the instability of ferroelectric domain switching. Our previous work has reported that the ferroelectric polarization of dopant-free HfO_2 can be significantly enhanced by mechanical stress of metal electrode [22], but also reveal the issues of interface traps and leakage current.

To solve those above these problems, we adopt the AlO_x capping layer to integrate with the ferroelectric $HfZrO_x$ film. The AlO_x film owns large bandgap and excellent thermal stability, which can offer a stable interface desirable for ferroelectric phase transition during high-temperature annealing process. The ferroelectric crystallinity, ferroelectric polarization property, leakage current characteristics and switching stability will be discussed here.

II. EXPERIMENTS

In this work, we fabricated dopant-free HfO_2 MFM capacitors with AlO_x CL. A 30-nm-thick TiN was grown as a bottom electrode on n^+-type Si substrate, then 7-nm-thick dopant-free HfO_2 was deposited on the bottom TiN electrode by thermal atomic layer process (ALD) using tetraethylmethyl amino hafnium (TDMAH) and H_2O precursor. After that, a 2-nm-thick AlO_x film using trimethylaluminum (TMA) and H_2O precursor was deposited on HfO_2 film as CL. After depositing AlO_x CL, the annealing temperature of 600°C was performed under nitrogen ambient for 30sec. Finally, the tantalum nitride (TaN) was deposited by sputtering system as a top electrode. The flow rates of Ar and N_2 are 100 sccm and 10 sccm, respectively. The area of MFM capacitor is 10000 μm^2. On the other hand, in order to investigate the CL effect of doped-HfO_2 MFM capacitors, the 7.5-nm-thick ferroelectric $HfZrO_x$ MFM capacitors with Zr-doping ratio of 50% using tetrakis (dimethylamido) zirconium (TDMAZ) and H_2O precursor were simultaneously fabricated. The selected thicknesses of AlO_x CLs for ferroelectric $HfZrO_x$ were 1 nm, 1.5 nm, and 2 nm. The polarization hysteresis loops and electrical characteristics of MFM capacitor devices were measured by using a precision RT66C ferroelectric tester and a semiconductor characterization system (Keithley 4200-SCS), respectively.

III. RESULTS AND DISCUSSION

Fig. 1(a) shows the polarization hysteresis loop of HfO_x MFM capacitors at an applied voltage of 2.5 V. It is clearly observed that the HfO_x MFM capacitor presents a weak ferroelectric property. This is because non-ferroelectric phase within HfO_x dominates the ferroelectric behavior of HfO_x MFM capacitor. To improve the ferroelectric property, a thin AlO_x film is introduced as a capping layer on HfO_x layer. From the polarization switching property, the well-behaved hysteresis loop is significantly enhanced after using amorphous AlO_x CL, which explain that the AlO_x CL plays a key role in determining the ferroelectric crystallinity and interface-trap formation during the annealing of HfO_x. The maximum doubled remanent polarization ($2P_r$) was shown in Fig. 1(b). The value of $2P_r$ measured at ±2.5 V increases from 1.3 to 6.2 $\mu C/cm^2$ after using AlO_x CL, which confirms the enhanced ferroelectric polarization under excluding the contribution of leakage current. To deeply understand the influence of AlO_x CL effect on the ferroelectricity of dopant-free HfO_x film, the film crystallinity of AlO_x/HfO_x film stack was analyzed by grazing-angle incidence x-ray diffraction (GI-XRD), as shown in Fig. 1(c). Compared to the control sample without CL, the HfO_x MFM capacitor with CL shows the significant increase in the peak (111) at 30.3° (orthorhombic phase) responsible for ferroelectric property. Moreover, the intensity of orthorhombic peak (020) at 35.6° is also stronger than that of control sample. Thus, it can be found that the monoclinic phase of control sample can be partially suppressed under capping layer effect, as shown in Fig. 1(d). The reduction on the monoclinic phase ratio from 67% to 54% is important for facilitating the orthorhombic phase transformation during film annealing. As seen Fig. 1(e), the increase of orthorhombic phase ratio from 32% to 45% is achieved with the assistance of AlO_x CL, which effectively provides enough ferroelectric domains in dopant-free HfO_x.

In order to understand the difference of AlO_x CL effect between dopant-free HfO_x and doped-HfO_x films, the $HfZrO_x$ MFM capacitors with different CL thicknesses were also carried out for a performance comparison. From thermodynamic analysis, the Gibbs free energies for ZrO_2, HfO_2, Al_2O_3 and TaN are −1100 kJ/mol, −1010.8 kJ/mol, −1500 kJ/mol, and −604.96 kJ/mol, respectively [23], [24]. We can understand that the interface reaction at the TaN/HfO_x and TaN/ZrO_x interface is more significant than that of TaN/AlO_x interface. Thus, the interface quality between TaN electrode and ferroelectric $HfZrO_x$ is a major concern for the stability of ferroelectric domain switching. The Fig. 2(a) shows the transmission electron microscope (TEM) images of $HfZrO_x$ films with 1-nm- and 2-nm-thick AlO_x CLs. The AlO_x CL is amorphous phase confirmed by fast Fourier transform (FFT) pattern of TEM image. Fig. 2(b) shows the hysteresis loops of $HfZrO_x$ MFM capacitors with different CL thicknesses. We can clearly observe that the ferroelectric polarization property is largely improved by AlO_x CL. With increasing the thickness of CL, the value of $2P_r$ increases from 11.9 $\mu C/cm^2$ to 36.9 $\mu C/cm^2$, which exhibits at least three times increase in $2P_r$. In addition, the case of 2 nm-CL has larger instantaneous current than other conditions as shown in Fig. 2(c).

The GI-XRD spectrum of $HfZrO_x$ MFM capacitors with different thicknesses of CLs were shown in Fig. 3(a). It can be seen that the intensities of peaks at 30.3° (111) and 35.6° (020) corresponding to orthorhombic phase enhances with the increase of AlO_x CL, especially for the case with a 2-nm-thick AlO_x CL. Thus, we can confirm the strong ferroelectricity observed in 2-nm-thick CL case is mainly originated from the increase of ferroelectric crystalline phase. As shown in Fig. 3(b), the orthorhombic phase ratios significantly increase from 48% to 57% under the optimal thickness condition of 2-nm-thick AlO_x CL. Compared to ferroelectric crystallization of dopant-free HfO_x shown in Fig. 1(e), the HfO_x film integrating with Zr doping and AlO_x capping layer can optimize the orthorhombic phase ratio up to 57% and maximize the $2P_r$ up to 36.9 $\mu C/cm^2$ at a low operating voltage of 3 V.

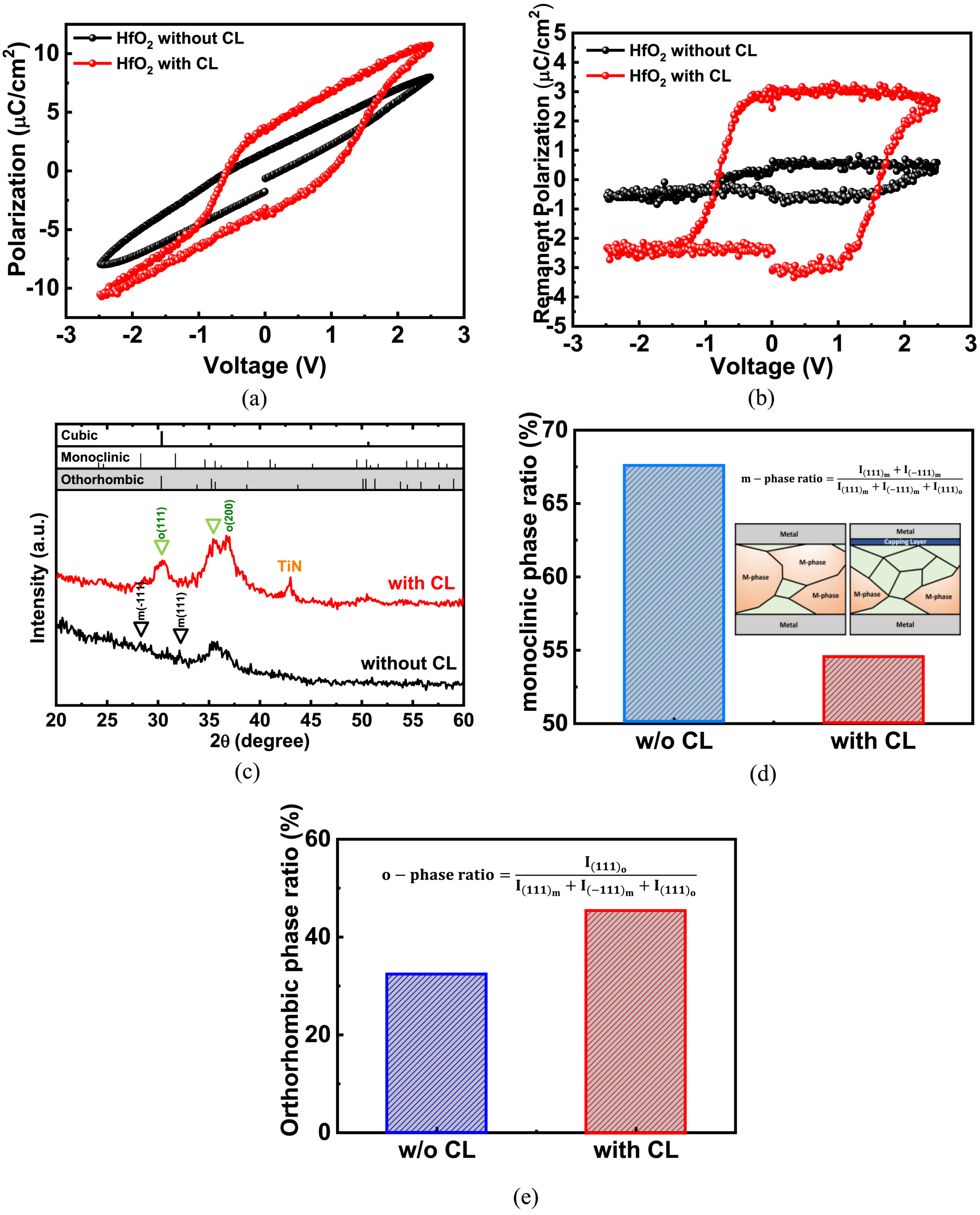

FIGURE 1. (a) Polarization-voltage characteristics, (b) remanent polarizaion and (c) GI-XRD spectrum of HfO_x MFM capacitors without and with AlO_x CLs. Capping layer thickness dependence of (d) monoclinc phase ratio and (e) orthorhombic phase ratio in HfO_x film without and with AlO_x CLs.

Fig. 4(a) shows the typical butterfly-shaped C-V curves measured from $HfZrO_x$ MFM capacitors with various thicknesses of CLs. The capacitance values measured at 100 kHz with bi-directional sweeps and showed significant increase as the thickness of AlO_x CL increase. The dielectric permittivity derived from *C-V* curves is shown in Fig. 4(b). The extracted permittivity of $HfZrO_x$ film without CL is ∼ 21 and the permittivity of $HfZrO_x$ with 2-nm-thick AlO_x CL is ∼ 29. It can be inferred that the AlO_x CL lowers the stray electric field and enhances the polarization electric field, which increases the permittivity of ferroelectric film stack [25]. Thus, the amorphous AlO_x CL has no adverse effect on the depolarization field due to the increase of orthorhombic phase stemming from capping effect to give rise to higher amount of switching domains, which fully agrees to the results of Fig. 2(a) and Fig. 3(b).

On the other hand, to understand the influence of interface traps on the leakage current characteristics of $HfZrO_x$ MFM

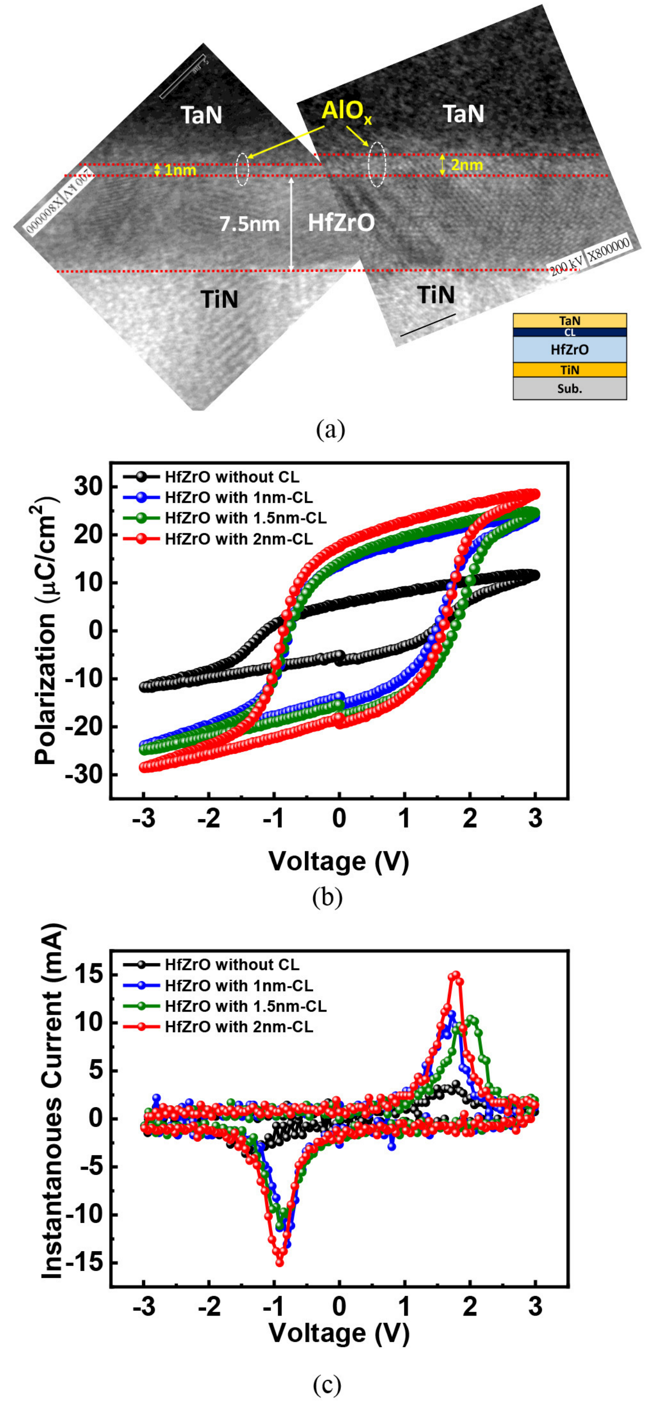

(a)

(b)

(c)

FIGURE 2. **(a) TEM image, (b) polarization-voltage characteristics, and (c) iinstantaneous current characteristics of HfZrO$_x$ MFM capacitors without and with AlO$_x$ CLs.**

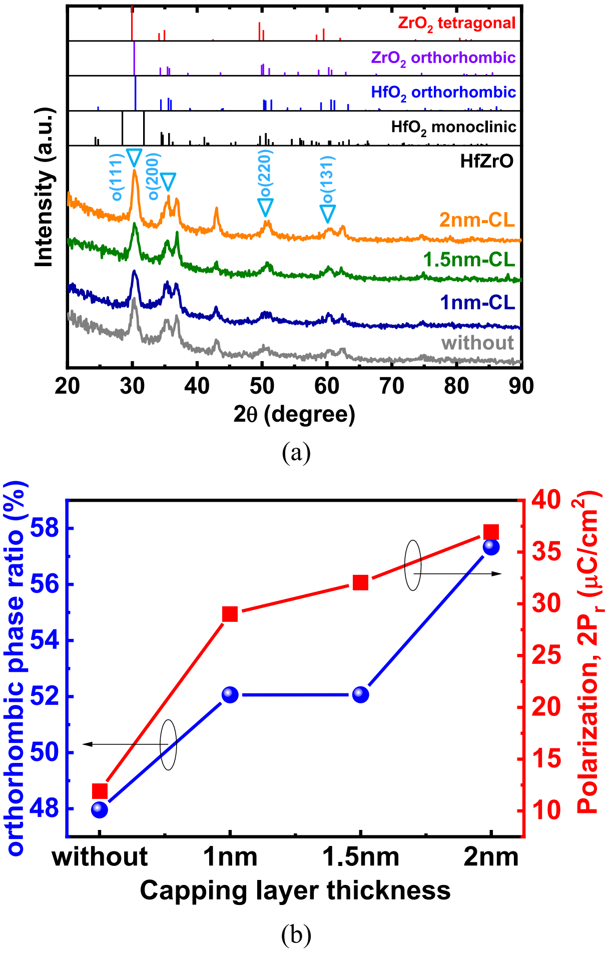

(a)

(b)

FIGURE 3. **(a) GI-XRD spectrum of HfZrO$_x$ MFM capacitors without and with AlO$_x$ CLs. (b) Capping layer thickness dependence of o-phsase ratio in HfZrO$_x$ film without and with AlO$_x$ CLs.**

capacitor before and after using AlO$_x$ CL, the temperature dependence of I-V measurement was also performed, as shown in Fig. 5(a). The leakage current at 2.5 V for HfZrO$_x$ MFM capacitor with AlO$_x$ CL is apparently lower than that of control sample without CL, especially at high temperature of 85°C. The leakage current at 85°C is effectively improved from 1.29×10^{-6} A to 9.55×10^{-8} A under the optimal thickness of 2-nm-thick AlO$_x$ CL. The high temperature leakage suppression can be ascribed to wide bandgap of AlO$_x$ with large conduction band offset with Si [26]. Fig. 5(b) presents the calculation result of the trapping level extracted from I-V curves of Fig. 5(a). It can be clearly observed that the trapping level gradually changes from 0.66 eV to 0.77 eV with increasing the CL thickness up to 2nm. The deeper trapping level of 0.77 eV is mainly ascribed to the effect of AlO$_x$ CL, which not only reduces the shallow traps near TaN/HfZrO$_x$ interface [27], [28], but also enhances the thermal stability of HfZrO$_x$ MFM capacitor. Therefore, the AlO$_x$ CL effectively improves interface quality to eliminate the interface shallow traps, possibly causing charge trapping/detrapping and domain wall pining during ferroelectric switching.

To further study the switching stability of HfZrO$_x$ MFM capacitors without and with AlO$_x$ CL, the endurance cycling test was performed under an applied voltage of 3V, as shown in Fig. 6. The wake-up process was performed under a pulse voltage of 3V at a frequency of 1 kHz. From the endurance characteristics, the HfZrO$_x$ MFM capacitor with CL is able to withstand 2.65×10^6 endurance cycles under repetitive field cycling. For the best condition of 2-nm-thick AlO$_x$ CL,

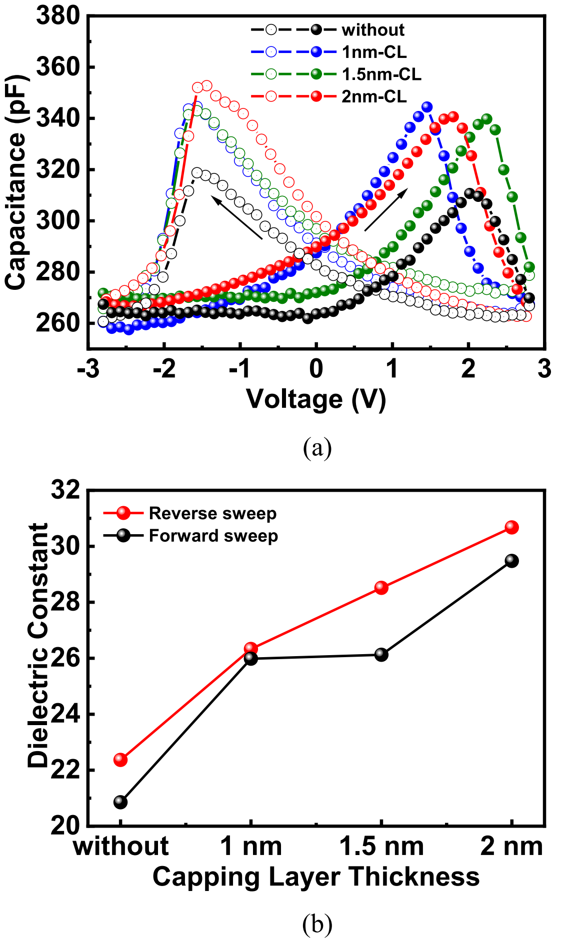

FIGURE 4. **(a) *C-V* characteristics of $HfZrO_x$ MFM capacitors without and with AlO_x CLs. (b) Capping layer thickness dependence of dieletric permittiivty of $HfZrO_x$ film.**

the $2P_r$ of 14.17 μC/cm^2 is still measured after 2.65×10^6 cycles, which presents significant improvement in $2P_r$ value and endurance cycle as compared to control sample without CL. By contrast, the $2P_r$ value measured at 10^6 cycles of $HfZrO_x$ MFM capacitor with CL is almost three time larger than that of control sample. The remarkable fatigue performance improvement is attributed to well-controlled interface quality between TaN electrode and ferroelectric $HfZrO_x$ due to the adoption of AlO_x CL, which alleviates the generation of defect traps and provides a reliable domain switching during long-term endurance cycling.

IV. CONCLUSION

In this work, we demonstrated the ferroelectric polarization characteristics of dopant-free HfO_x and $HfZrO_x$ MFM capacitors with AlO_x CLs. For dopant-free HfO_x film, the AlO_x CL effectively reduces the formation of monocline phase within HfO_x and promotes the ferroelectric phase transition during annealing. Furthermore, the ferroelectricity, leakage current and endurance cycling of $HfZrO_x$ MFM capacitors are also largely improved after using AlO_x CLs. These improvements are due to the contribution of interface engineering to obtain enhanced ferroelectric crystallinity and well-controlled interface with remarkably deeper trapping level than control sample.

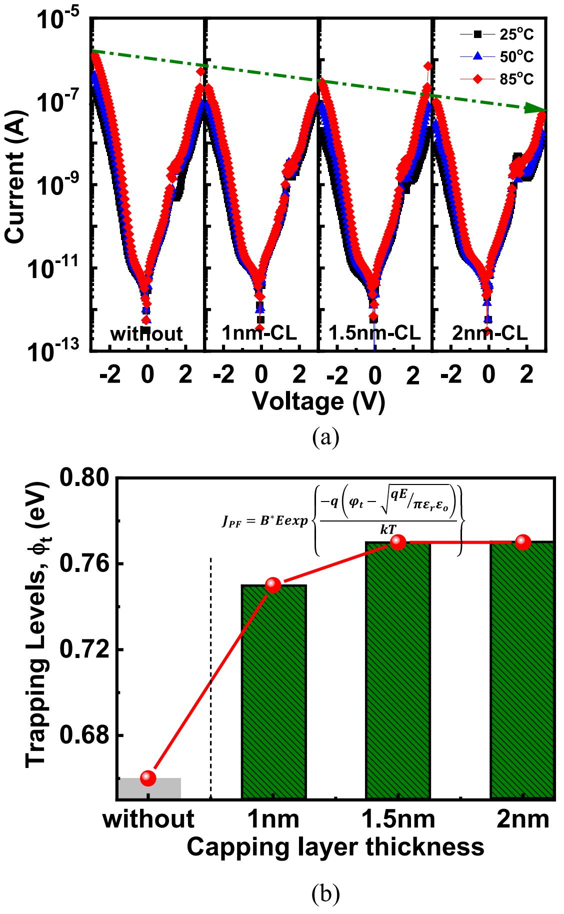

FIGURE 5. **(a) Temperature dependence of *I-V* characteristics of $HfZrO_x$ MFM capacitors without and with AlO_x CLs. (b) Capping layer thickness dependence of trapping levels (φ_t) in $HfZrO_x$ MFM capacitors.**

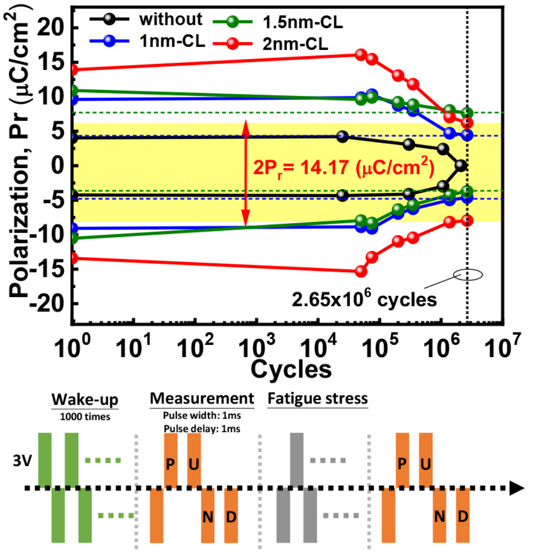

FIGURE 6. **Endurance cycling characteristics of $HfZrO_x$ MFM capacitors without and with AlO_x CLs.**

REFERENCES

[1] T. Hiramoto et al., “Ultra-low power and ultra-low voltage devices and circuits for IoT applications,” in *Proc. IEEE Silicon Nanoelectron. Workshop*, Jun. 2016, pp. 146–147, doi: 10.1109/SNW.2016.7578025.

[2] C. C. Fan et al., “Program/erase speed and data retention trade-off in negative capacitance versatile memory,” in *Proc. Silicon Nanoelectron. Workshop*, Jun. 2017, pp. 101–102, doi: 10.23919/SNW.2017.8242317.

[3] K. T. Chen et al., “Non-volatile ferroelectric FETs Using 5-nm $Hf_{0.5}Zr_{0.5}O_2$ with high data retention and read endurance for 1T memory applications,” *IEEE Electron Device Lett.*, vol. 40, no. 3, pp. 399–402, Mar. 2019, doi: 10.1109/LED.2019.2896231.

[4] J. D. Luo et al., “Ferroelectric undoped HfO_x capacitor with symmetric synaptic for neural network accelerator,” *IEEE Trans. Electron Devices*, vol. 68, no. 3, pp. 1374–1377, Mar. 2021, doi: 10.1109/TED.2021.3052428.

[5] C. H. Cheng and A. Chin, “Low-leakage-current DRAM-like memory using a one-transistor ferroelectric MOSFET with a Hf-based gate dielectric,” *IEEE Electron Device Lett.*, vol. 35, no. 2, pp. 138–140, Jan. 2014, doi: 10.1109/LED.2013.2290117.

[6] M. H. Lee et al., “Steep slope and near non-hysteresis of FETs with antiferroelectric-like HfZrO for low-power electronics,” *IEEE Electron Device Lett.*, vol. 36, no. 4, pp. 294–296, Apr. 2015, doi: 10.1109/LED.2015.2402517.

[7] Y. C. Chiu, C. Y. Cheng, S. S. Yen, C. C. Fan, and H. H. Hsu, “On the variability of threshold voltage window in gate-injection versatile memories with Sub-60mV/dec subthreshold swing and 10^{12}-cycling endurance,” in *Proc. IEEE Int. Rel. Phys. Symp.*, Apr. 2016, pp. MY-7-1–MY-7-5, doi: 10.1109/IRPS.2016.7574623.

[8] C. H. Cheng, Y. C. Chiu, and G. L. Liou, “Experimental observation of negative capacitance switching behavior in one-transistor ferroelectric versatile memory,” *Physica Status Solidi-Rapid Res. Lett.*, vol. 11, no. 10, Aug. 2017, Art. no. 1700098, doi: 10.1002/pssr.201700098.

[9] Y. C. Chiu, C. H. Cheng, C. Y. Chang, Y. T. Tang, and M. C. Chen, “Investigation of strain-induced phase transformation in ferroelectric transistor using metal-nitride gate electrode,” *Physica Status Solidi-Rapid Res. Lett.*, vol. 11, no. 3, 2017, Art. no. 1600368, doi: 10.1002/pssr.201600368.

[10] C. C. Fan, C. H. Cheng, Y. R. Chen, C. Liu, and C. Y. Chang, “Energy-efficient $HfAlO_x$ NCFET: Using gate strain and defect passivation to realize nearly hysteresis- free sub-25mV/dec switch with ultralow leakage,” in *Proc. IEEE Int. Electron Devices Meeting*, Dec. 2017, pp. 23.2.1–23.2.4, doi: 10.1109/IEDM.2017.8268444.

[11] C. Liu et al., “High performance negative capacitance field-effect transistor featuring low off-state current, high on/off current ratio, and steep Sub-60 mV dec^{-1} swing,” *Jpn. J. Appl. Phys.*, vol. 59, no. SG, Jan. 2020, Art. no. SGGA01, doi: 10.7567/1347-4065/ab6420.

[12] C. Liu et al., “Gamma-ray irradiation effect on ferroelectric devices with hafnium aluminum oxides,” *Physica Status Solidi-Rapid Res. Lett.*, vol. 13, no. 12, Sep. 2019, Art. no. 1900414, doi: 10.1002/pssr.201900414.

[13] C. Liu et al., “Stabilizing ferroelectric domain switching of hafnium aluminum oxide using metal nitride electrode engineering,” *ECS J. Solid State Sci. Technol.*, vol. 8, bo. 10, p. 553, Sep. 2019, doi: 10.1149/2.0041910jss.

[14] C. H. Cheng et al., “Investigation of gate-stress engineering in negative capacitance FETs Using ferroelectric hafnium aluminum oxides,” *IEEE Trans. Electron Devices*, vol. 66, no. 2, pp. 1082–1086, Feb. 2019, doi: 10.1109/TED.2018.2888836.

[15] C. H. Cheng et al., “Impact of zirconium doping on steep subthreshold switching of negative capacitance hafnium oxide based transistors,” *Physica Status Solidi-Rapid Res. Lett.*, vol. 13, no. 5, May 2019, Art. no. 1800573, doi: 10.1002/pssr.201800573.

[16] M. H. Lin et al., “On the electrical characteristics of ferroelectric finfet using hafnium zirconium oxide with optimized gate stack,” *ECS J. Solid State Sci. Technol.*, vol. 7, no. 11, pp. 640–646, Oct. 2018, doi: 10.1149/2.0091811jss.

[17] K. T. Chen et al., “Ferroelectric $HfZrO_2$ FETs for steep switch onset,” *Microelectron. Eng.*, vol. 215, no. 15, Art. no. 110991, 2019, doi: 10.1016/j.mee.2019.110991.

[18] S. Zarubin et al., “Fully ALD-grown TiN/$Hf_{0.5}Zr_{0.5}O_2$/TiN stacks: Ferroelectric and structural properties,” *Appl. Phys. Lett.*, vol. 109, no. 19, 2016, Art. no. 192903, doi: 10.1063/1.4966219.

[19] A. Chernikova, M. Kozodaev, A. Markeev, Y. Matveev, D. Negrov, and O. Orlov, “Confinement-free annealing induced ferroelectricity in $Hf_{0.5}Zr_{0.5}O_2$ thin films,” *Microelectron. Eng.*, vol. 147, no. 1, pp. 15–18, 2015, doi: 10.1016/j.mee.2015.04.024.

[20] Y. C. Chiu, C. H. Cheng, C. Y. Chang, Y. T. Tang, and M. C. Chen, “One-transistor ferroelectric versatile memory: Strained-gate engineering for realizing energy-efficient switching and fast negative-capacitance operation,” in *Proc. IEEE Symp. VLSI Technol.*, Jun. 2016, pp. 1–2, doi: 10.1109/VLSIT.2016.7573414.

[21] Y. C. Chiu, C. H. Cheng, G. L. Liou, and C. Y. Chang, “Energy-efficient versatile memories with ferroelectric negative capacitance by gate-strain enhancement, ative capacitance FETs using ferroelectric hafnium aluminum oxides,” *IEEE Trans. Electron Devices*, vol. 64, no. 8, pp. 3498–3501, Aug. 2017, doi: 10.1109/TED.2017.2712709.

[22] C. H. Cheng, C. C. Fan, C. Y. Tu, H. H. Hsu, and C. Y. Chang, “Implementation of dopant-free hafnium oxide negative capacitance field-effect transistor,” *IEEE Trans. Electron Devices*, vol. 66, no. 1, pp. 825–828, Jan. 2019, doi: 10.1109/TED.2018.2881099.

[23] M. Ismail, Z. Batool, K. Mahmood, A. M. Rana, B. D. Yang, and S. Kim, “Resistive switching characteristics and mechanism of bilayer HfO_2/ZrO_2 structure deposited by radio-frequency sputtering for non-volatile memory,” *Results Phys.*, vol. 18, Sep. 2020, Art. no. 103275, doi: 10.1016/j.rinp.2020.103275.

[24] J. Guo et al., “Influence of nitrogen adsorption of doped Ta on characteristics of SiNx-based resistive random access memory,” *Physica Status Solidi-Rapid Res. Lett.*, vol. 216, no. 22, Sep. 2019, Art. no. 1900540, doi: 10.1002/pssa.201900540.

[25] A. K. Saha, M. Si, K. Ni, S. Datta, P. D. Ye, and S. K. Gupta, “Ferroelectric thickness dependent domain interactions in FEFETs for memory and logic: A phase-field model based analysis,” in *Proc. IEEE Int. Electron Devices Meeting*, Dec. 2020, pp. 4.3.1–4.3.4, doi: 10.1109/IEDM13553.2020.9372099.

[26] J. Kolodzey et al., “Electrical conduction and dielectric breakdown in aluminum oxide insulators on silicon,” *IEEE Trans. Electron Devices*, vol. 47, no. 1, pp. 121–128, Jan. 2000, doi: 10.1109/16.817577.

[27] W. Zhu et al., “HfO/sub 2/ and HfAlO for CMOS: Thermal stability and current transport,” in *Int. Electron Devices Meeting Tech. Dig.*, Dec. 2001, pp. 20.4.1–20.4.4, doi: 10.1109/IEDM.2001.979541.

[28] M. N. U. Bhuyian and D. Misra, “Multilayered ALD HfAlOx and HfO_2 for high-quality gate stacks,” *IEEE Trans. Device Mater. Rel.*, vol. 15, no. 2, pp. 229–235, Jun. 2015, doi: 10.1109/TDMR.2015.2424151.